

Effects of annealing on ZnS films produced by CBD method

Özlem YILMAZ¹ , Sevda İLDAN ÖZMEN^{2,*} , Hülya METİN GÜBÜR¹ 

¹Mersin University, Faculty of Science, Department of Physics, Mersin/TURKEY

²Mersin University, Advanced Technology Education Research and Application Center, Mersin/TURKEY

Abstract

The Zinc Sulfide (ZnS) thin films were produced at 60 °C on glass slides with the chemical bath deposition (CBD) method. The ZnS films were annealed for 1 hour at different temperatures in the air atmosphere. UV-visible spectrophotometer, X-ray diffraction (XRD), scanning electron microscope (SEM), energy dispersive X-ray spectroscopy (EDS), four-point probe technique and Hall-effect measurement techniques were used to examine the thermal annealing's effect on the films' optical, structural, and electrical properties. It was observed that with increased annealing temperature, the film thickness increased and thus the energy band gap decreased. It was seen that the particle size of the ZnS films grew depending on the annealing temperature, and the crystal structure turned into an amorphous structure. Finally, it was determined that with the impact of annealing the carrier type did not change, and the conductivity of the ZnS thin films increased.

Article info

History:

Received:03.05.2021

Accepted:24.08.2021

Keywords:

ZnS,
Chemical bath
deposition,
SEM,
Optical properties,
Hall Effect.

1. Introduction

Zinc sulfide with ZnS chemical formula is an important chalcogenide that belongs to the II-VI semiconductor family (e.g., CdSe, ZnSe, CdS, ZnS) [1–3]. Because of its wide fields of application such as optoelectronic devices, optical coatings, solar cells and light-emitting diodes, the ZnS thin films have been extensively studied. The thin film of zinc sulfide (ZnS), which has direct bandgap energies range from 3.50-3.70 eV at room temperature, is used for the semiconductor layers of solar cells and other technological devices [4–6]. ZnS is used as a buffer layer in CIGS, ZCTSSe, and CdTe cells since it has n-type conductivity due to a sulfur deficiency defect [7]. This material with a high refractive index (2.25-2.35) is found in cubic (zinc blende) and hexagonal (wurtzite) crystal structures [8, 9]. It is also an attractive material since it is environmentally friendly, inexpensive and flexible [10, 11].

Due to the importance of the functional properties of nanoscale materials, various techniques have been used to produce nanostructured ZnS semiconductors [12]. Synthesis techniques such as molecular beam epitaxy, thermal evaporation, RF sputtering, chemical bath deposition are used to deposit ZnS thin films [3, 6, 8, 10, 12]. Among these techniques CBD is the low

costly technique, it is easily deposited to wide areas and it is a simple technique that not need special equipment [3, 13, 14].

In this study, the ZnS nanocrystalline thin films were produced on glass slides with the CBD method at 60 ± 2 °C. The obtained ZnS films were annealed in the air atmosphere for 1 hour at temperatures of 150 °C, 250 °C and 350 °C. The optical, structural, and electrical properties of the nanocrystalline films were also examined.

2. Materials and Methods

2.1. Experimental details

0.050 M zinc sulphate (ZnSO₄), 25% ammonia (NH₃) / ammonium chloride (NH₄Cl), 1 M triethanolamine (C₆H₁₅NO₃), 0.050 M thioacetamide (C₂H₅NS) were prepared in an aqueous solution (pH = 10.8) at room temperature to obtain ZnS thin films. The solution was put into a water bath of 60 ± 2 °C which was placed on the hot plate. Glass slides for ZnS thin films were used as the substrate. Before coating, the glass substrates were cleaned with chromic acid, deionized pure water, propanol, and ethanol, respectively. Later, for a few minutes, an air dryer was used to dry them. The clean substrates were then positioned at a 45 °

*Corresponding author. e-mail address: sevdaildan@mersin.edu.tr
<http://dergipark.gov.tr/cs.j> ©2021 Faculty of Science, Sivas Cumhuriyet University

angle in a beaker containing 100 ml deposition mixture and held for 1h at 60°C without stirring. The bath temperature was controlled by a thermometer. The deposition of ZnS semiconductor thin films was repeated sixteen times for 1h duration time on the same substrate and each time the chemical bath solution was refreshed. The ZnS films were etched in 5% HF solution to remove the loosely adhered ZnS particles on the film surface, then washed with propanol and finally dried in air. At the end of the deposition, four identical 250 nm thick films were obtained and these nanocrystalline films were annealed at 150 °C, 250 °C, and 350 °C temperatures in an air atmosphere.

3. Results and Discussion

3.1. Optical properties

The transmission spectra in the wavelength range of 300-1100 nm of the ZnS films were used to record

using a UV-visible spectrophotometer. The thickness of the films was calculated from the transmission interference using the following equation,

$$t = \frac{1}{2n \left(\frac{1}{\lambda_2} - \frac{1}{\lambda_1} \right)} \quad (1)$$

where t is the film thickness, n is refractive index, and λ_1 and λ_2 are adjacent maxima or minima of the transmission spectra [15]. The absorption coefficients were calculated by Beer-Lambert law using the transmission spectrum.

$$\alpha = A(h\nu - E_g)^n / h\nu \quad (2)$$

where A is a constant, α is absorption coefficient, $h\nu$ is the photon energy and n is also a constant, equal to 1/2 for direct band gap semiconductor [16].

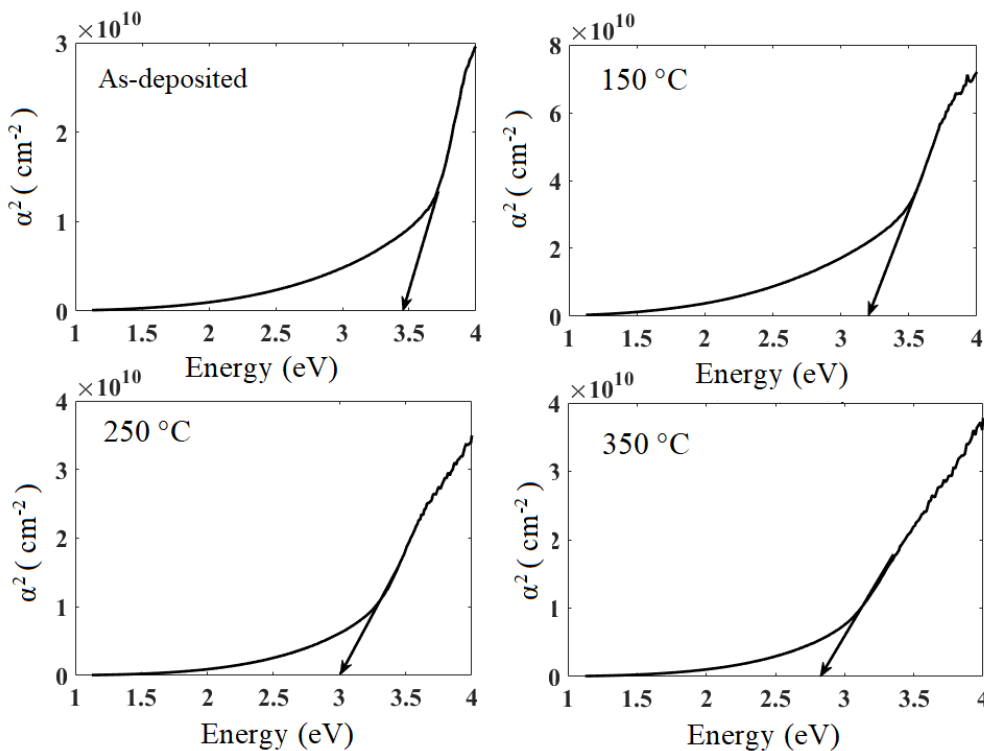


Figure 1. The α^2 versus photon energy of the ZnS films.

The band gap energy (E_g) is the energy value where $\alpha^2 = 0$ as shown in the energy versus absorption ($\alpha^2-h\nu$) graphs in Figure 1. The band gap energy and thickness changes of as-deposited and annealed ZnS films depending on annealing temperature are shown in Figure 2. It was seen that as the film annealing temperature was raised, the optical absorption in the forbidden zone decreased and the film thickness

increased. This property suggests that as the annealing temperature is raised, the film quality is improved. The optical absorption in the band-to-band region is also seen to decrease with the film annealing temperature. Since the size of the inter-granular empty space in the films increases as the annealing temperature increases, the density of the film decreases (lower α values). Optical scattering was also observed changes with

annealing temperature and this change was seen from the long-wavelength region in the absorption graph. The E_g of the as-deposited film (3.48 eV) is nearly identical to that of bulk ZnS (3.67 eV) [17, 18]. The optical absorption of films (at 150 °C, 250 °C and 350 °C) becomes sharper in the 300-400 nm wavelength region with annealing. Here, it is possible to identify the excitonic absorption. In the same region, the as-deposited film gives a broadened absorption spectrum. This observation can be explained as follows. In thinner films, the excitonic absorption/bulk absorption ratio is greater than thicker films, so the excitonic absorption can be observed much more easily. As the thicknesses of the films decrease, the ratio of surface to volume increases. A hole at the surface has a lower probability of catching an electron than a hole in the bulk. So, we expect that thinner films would show significant excitonic absorption than thicker films.

3.2. Morphological properties

The surface morphology of the ZnS nanocrystalline thin films was investigated in the SEM images, recorded with a Zeiss-Supra 55 SEM equipped with an energy dispersive X-ray (EDS) spectrometer. The SEM images in Figure 3 show that the samples are free of impurities and structural defects. The morphology, grain structure, and surface characteristics of the ZnS samples obtained at temperatures 150, 250 and 350 °C were almost similar. It can also be seen in Figure 3 that small spherical nanosized ZnS grains were well-deposited and homogeneous on the glass substrate. It was observed with increasing annealing temperature that the bigger particles are formed. This growth of particle size of the ZnS thin films is due to particle coalescence. The elemental ratio Zn : S was found to be more than three times higher (Zn : S elemental percentage ratio 77 : 23) in the quantitative analysis of the as-deposited ZnS thin film made with EDS and EDS graph is shown in Figure 4.

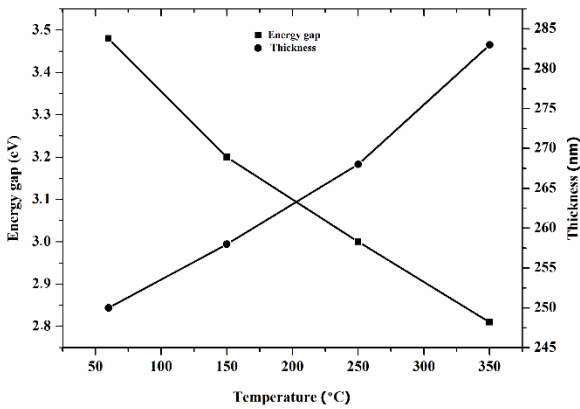


Figure 2. Temperature dependence of the thickness and energy gap of the ZnS films.

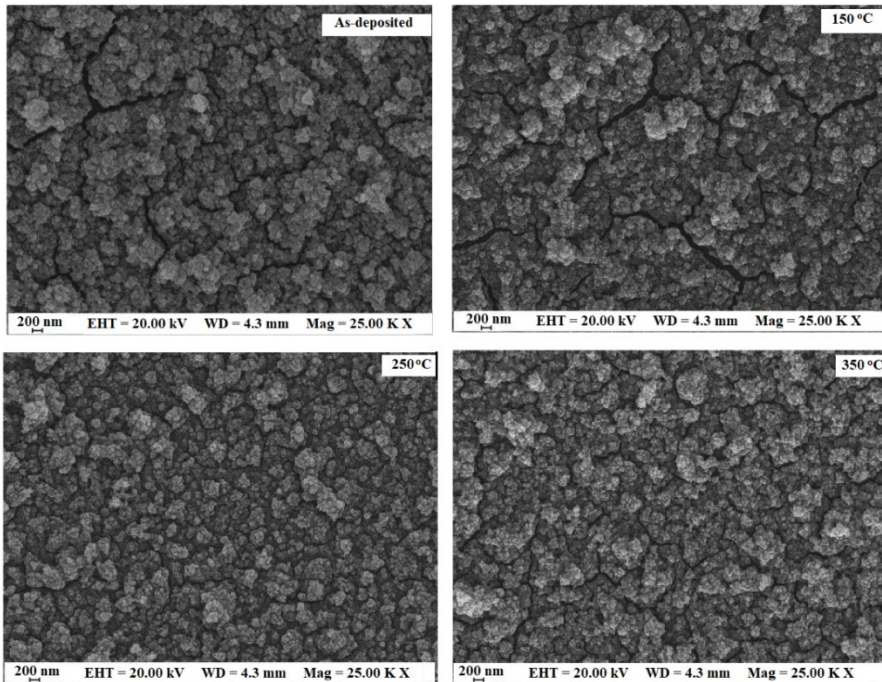


Figure 3. The SEM images of the ZnS films at different temperatures.

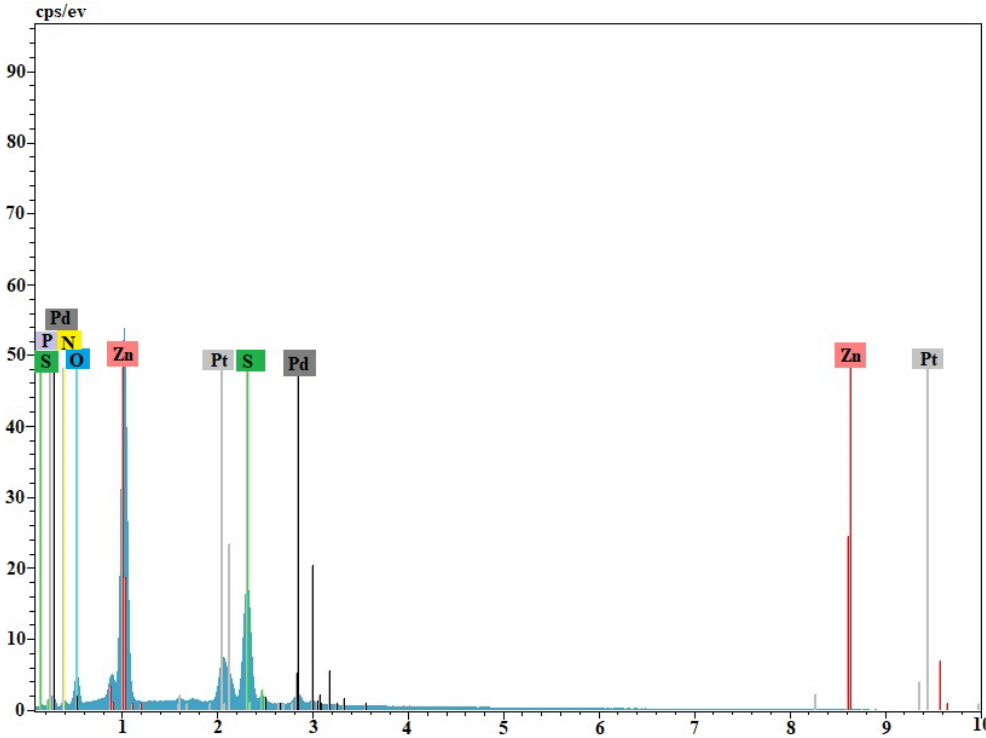


Figure 4. The EDS graph of the as-deposited ZnS films.

3.3. Structural properties

The structural properties of ZnS nanocrystalline thin films were investigated by Rigaku Smart Lab X-ray diffractometer using $\text{CuK}\alpha$ radiation ($\lambda = 1.54 \text{ \AA}$). The XRD graph of the as-deposited and annealed ZnS films is shown in Figure 5. Figure 5 shows that although there was a peak at the as-deposited film, this peak was lost at the annealed films. The plane indices of the observed “d” are obtained, by using the standard value of the “d” for the ZnS thin films, which are given by hexagonal (H) (JPDFS Card No: 01-074-5002). The standard “d” values are in good agreement with the observed “d” values of the as-deposited ZnS. When the images of the annealed ZnS thin films were investigated, it was seen that broadening in the diffraction peaks of the films. This is due to the existence of nanosized materials. No peak was observed at annealed films because all films were amorphous, as seen in earlier studies [14, 19].

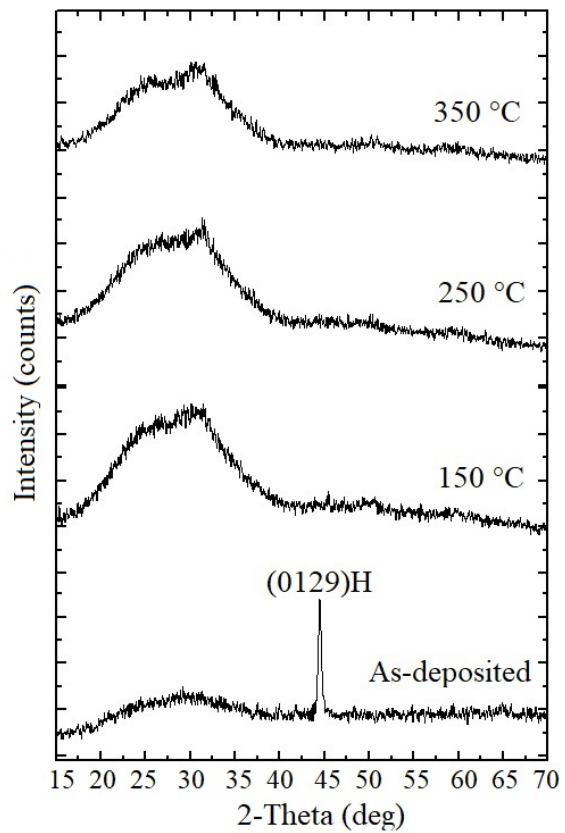


Figure 5. X-ray diffractograms of the as-deposited and the annealed ZnS films at different temperatures.

3.4. Electrical properties

The electrical conductivity of the ZnS nanocrystalline thin films was measured as a function of temperature in the range of 50-400 °C using the four-point probe technique. The resistivity and conductivity were determined as described in our previous publication [16].

Figure 6 shows the conductivity of the films as a function of temperature. The conductivity values are between 10^{-6} – 10^{-5} (Ω - cm)⁻¹ at the temperature range of 50-400 °C as seen in Figure 6. The conductivity of as-deposited and annealed (at 150 °C, 250 °C and 350 °C) films increases exponentially with the increasing

temperature, as is typical semiconductors. There are two distinct conductivity regions in Figure 6. Activation energies can be calculated using these regions. For this, the activation energy E_a of the ZnS films has been calculated by $\sigma = \sigma_o \exp(-E_a / k_B T)$ equation, where σ is the conductivity of the films, σ_o is the pre-exponential factor, E_a is activation energy, k_B is Boltzmann constant and T is temperature. The activation energy values of the films were calculated for two distinct temperature regions such as low temperature region (LT) ($40 \text{ }^\circ\text{C} \leq T \leq 250 \text{ }^\circ\text{C}$) and high temperature region (HT) ($250 \text{ }^\circ\text{C} \leq T \leq 400 \text{ }^\circ\text{C}$). Calculated values were shown in Table 1.

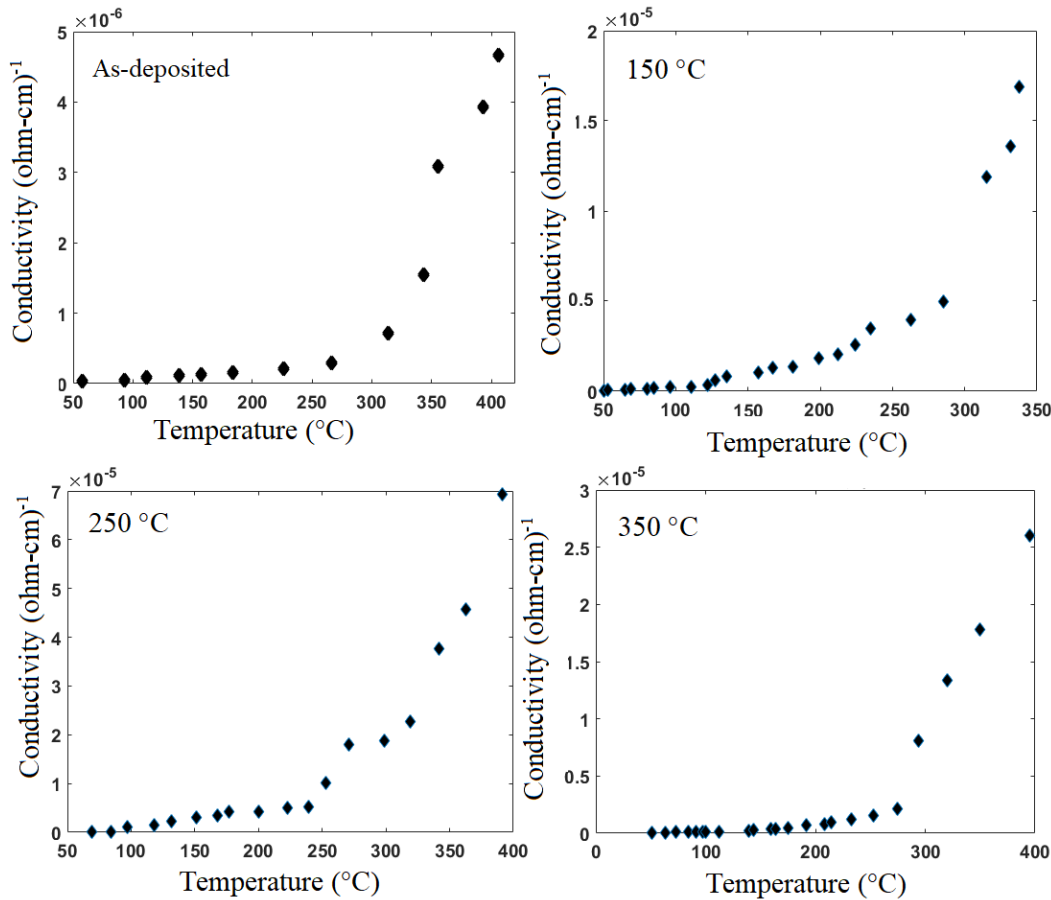


Figure 6. Temperature dependence of the electrical conductivity of the as-deposited and annealed ZnS films.

Table 1. The activation energies of the ZnS films.

| Annealing temperature (°C) | LR (meV) | HR (meV) |
|----------------------------|----------|----------|
| As-deposited | 10.00 | 29.00 |
| 150 | 20.00 | 23.00 |
| 250 | 15.00 | 25.00 |
| 350 | 14.00 | 30.00 |

LR: Low temperature region and HR: High temperature region

Except for the four-point probe technique, we used the Hall effect method to better understand the electrical properties. By this method, the electrical properties of the ZnS films were determined at room temperature using a Hall effect measurement generated by the Van der Pauw geometry. Hall effect measurements were performed by making ohmic contacts on four corners of the ZnS films. The magnitude of the magnetic field and current values were taken as 0.54 Tesla and 1 mA, respectively. Hall measurements for each sample were

repeated several times to ensure the reliability of the results.

The Hall effect measurements accomplished for as-deposited and annealed ZnS films are given in Table 2. All of the ZnS thin films that were as-deposited and annealed were n-type materials. With increasing annealing temperature, there was no significant change in carrier concentration and resistivity. It was observed

that the resistivity of the ZnS films were very low due to the excess of Zn in the structure. The higher mobility of the annealed ZnS films can be explained by the increasing grain size which was caused that annealing. Similar results have been given in previous work [20–24].

Table 2. The Hall Effect measurements of the ZnS films.

| Annealing temperature (°C) | Carrier concentration (cm ⁻³) | Mobility (cm ² /Vs) | Resistivity (Ω - cm) | Carrier type |
|----------------------------|---|--------------------------------|-------------------------|--------------|
| As-deposited | 1.526 x 10 ¹² | 4.768 x 10 ¹ | 8.576 x 10 ⁴ | n |
| 150 | 1.147 x 10 ¹³ | 6.551 x 10 ⁰ | 8.311 x 10 ⁴ | n |
| 250 | 1.835 x 10 ¹² | 4.344 x 10 ¹ | 7.832 x 10 ⁴ | n |
| 350 | 1.351 x 10 ¹² | 6.142 x 10 ¹ | 7.523 x 10 ⁴ | n |

4. Conclusions

The optical results of the ZnS films show that as the annealing temperature was increased, the film thickness increased, and the band gap energy (E_g) decreased from 3.36 to 2.82 eV. The grain structure and surface properties of as-deposited and annealed ZnS nanocrystalline films, which were coated well and homogeneously on the glass substrate and composed of small spherical nanoscale particles, were shown by SEM images of the films. It was also observed that the grain size increased for ZnS thin films and intergranular cavities increased with the increasing annealing temperature. XRD data showed that all of the annealed films were in the amorphous phase. The ZnS thin films were determined to be n-type using Hall measurements, and the carrier type did not change as the annealing temperature increased. In addition, it was observed in the four-point probe measurement data with increasing annealing temperature that the conductivity increased and the resistivity decreased, as seen in semiconductors. Considering all of these findings, it's possible to say that ZnS films might be used as buffer layers in CIGS solar cells.

Acknowledgment

This study was supported by the Scientific Research Project Fund of Mersin University with Project Numbers: 2017-2-TP3-2593 and 2017-2-TP2-2573. The authors would like to thank the Mersin

University Advanced Technology Education Research and Application Center (MEİTAM) for its technical support and Prof. Dr. Ramazan Esen for the Hall measurements.

Conflicts of interest

Sample sentences if there is no conflict of interest: The authors state that did not have conflict of interests.

References

- [1] Ojo A. A., Influence of electroplating temperature on the characteristic properties of zinc sulphide, *Mater. Res. Express*, 6 (2019).
- [2] Igweoko A. E., Augustine C., Idenyi N. E., Okorie B. A., Anyaegbunam F. N. C., Influence of processing conditions on the optical properties of chemically deposited zinc sulphide (ZnS) thin film, *Mater. Res. Express*, 5 (2018).
- [3] Nabiyouni G., Sahraei R., Toghiani M., Ara M. H. M., Hedayati K., Preparation and characterization of nanostructured ZnS thin films grown on glass and N-type Si substrates using a new chemical bath deposition technique, *Rev. Adv. Mater. Sci.*, 27 (2011) 52–57.
- [4] Metin H., Esen R., Changes on the Structural and Optical Properties of ZnS Films by Chemical Bath

Deposition Technique on Annealing in Air Atmosphere, *Cumhur. Univ. Fac. Arts Sci. - J. Sci.*, 28 (3) (2003) 82–91.

- [5] Xie Y. et al., Improving performance in CdTe/CdSe nanocrystals solar cells by using bulk nano-heterojunctions, *J. Mater. Chem. C*, 4 (2016) 6483–6491.
- [6] Zhou L., Tang N., Wu S., Hu X., Xue Y., Influence of deposition time on ZnS thin films performance with chemical bath deposition, *Phys. Procedia*, 22 (2011) 354–359.
- [7] Ortega-Cardenas J. A., Albor-Aguilera M. L., Hernabdez-Vasquez C., Impact of different thermal treatments on ZnS physical properties and their performance in CdTe solar cells, *Mater. Res. Express*, 6 (8) (2019).
- [8] Haddad H., Chelouche A., Talantikite D., Merzouk H., Boudjouan F., Djouadi D., Effects of deposition time in chemically deposited ZnS films in acidic solution, *Thin Solid Films*, 589 (2015) 451–456.
- [9] Arenas O. L., Nair M. T. S., Nair P. K., Chemical bath deposition of ZnS thin films and modification by air annealing, *Semicond. Sci. Technol.*, 12 (1997) 1323–1330.
- [10] Göde F., Güneri E., Kariper A., Ulutaş C., Kirmizigül F., Gümüş C., Influence of annealing temperature on the structural, optical and electrical properties of amorphous Zinc Sulfide thin films, 17th International Conference on Microscopy of Semiconducting Materials 2011- Journal of Physics: Conference Series, 2011.
- [11] Nwofe P. A., Robert B. J., Agbo P. E., Influence of processing parameters on the structural and optical properties of chemically deposited Zinc Sulphide thin films, *Mater. Res. Express*, 5 (10) (2018).
- [12] Talantikite-Touati D., Merzouk H., Haddad H., Tounsi A., Effect of dopant concentration on structural and optical properties Mn doped ZnS films prepared by CBD method, *Optik*, 136 (2017) 362–367.
- [13] Jobzari H. G., Iranmanesh P., Sabet M., Saeednia S., Effect of synthesis method and chemical reagents on the structural parameters, particle size, and optical and photoluminescence properties of ZnS nanostructures, *Luminescence*, (2019) 1-10.
- [14] Nikzad M., Khanlary M. R., Rafiee S., Structural , optical and morphological properties of Cu -doped ZnS thin films synthesized by sol – gel method, *Appl. Phys. A Mater. Sci. Process.*, 125 (507) (2019).
- [15] Pankove J. I., Optical Processes in Semiconductors. New York: Dover Publications, (1971).
- [16] Metin H., Erat S., Arı M., Bozoklu M., Characterization of CdSe films prepared by chemical bath deposition method, *Optoelectron. Adv. Mater. Rapid Commun.*, 2 (2) (2008) 92–98.
- [17] Yang K., Li B., Zeng G., Effects of temperature on properties of ZnS thin films deposited by pulsed laser deposition, *Superlattices Microstruct.*, 130 (2019) 409–415.
- [18] Liang G., Fan P., Chen C., Luo J., Zhao J., Zhang D., Improved microstructure and properties of CBD-ZnS thin films, *J. Mater. Sci. Mater. Electron.*, 26 (2015) 2230–2235.
- [19] Wei A., Liu J., Zhuang M., Zhao Y., Preparation and characterization of ZnS thin films prepared by chemical bath deposition, *Mater. Sci. Semicond. Process.*, 16, (6) (2013) 1478–1484.
- [20] Bakiyaraj G., Gopalakrishnan N., Dhanasekaran R., Influences of thermal annealing on the structural, optical and electrical properties of nanostructured cadmium sulphide thin films, *Chalcogenide Lett.*, 8 (7), (2011) 419–426.
- [21] Erdogan N. H., Kara K., Ozdamar H., Esen R., Kavak H., Effect of the oxidation temperature on microstructure and conductivity of Zn x N y thin films and their conversion into p-type ZnO:N films, *Appl. Surf. Sci.*, 271 (2013) 70–76.
- [22] Khallaf H., Oladeji I. O., Chow L., Optimization of chemical bath deposited CdS thin films using nitrilotriacetic acid as a complexing agent, *Thin Solid Films*, 516 (2008) 5967–5973.
- [23] Liu F. et al., Characterization of chemical bath deposited CdS thin films at different deposition temperature, *J. Alloys Compd.*, 493 (2010) 305–308.

- [24] Kose S., Atay F., Bilgin V., Akyuz I., Ketenci E., Optical characterization and determination of carrier density of ultrasonically sprayed CdS:Cu films, *Appl. Surf. Sci.*, 256 (2010) 4299–4303.